Video Article

Diagnostic Ultrasound Imaging of Mouse Diaphragm Function

Li Zuo[1,2], William J. Roberts[1,2], Kevin D. Evans[1]

[1]Radiologic Sciences & Respiratory Therapy Division, School of Health and Rehabilitation Sciences, Davis Heart and Lung Research Institute, The Ohio State University College of Medicine

[2]Department of Biological Sciences, Oakland University

Correspondence to: Li Zuo at zuo.4@osu.edu

Abstract

Function analysis of rodent respiratory skeletal muscles, particularly the diaphragm, is commonly performed by isolating muscle strips using invasive surgical procedures. Although this is an effective method of assessing *in vitro* diaphragm activity, it involves non-survival surgery. The application of non-invasive ultrasound imaging as an *in vivo* procedure is beneficial since it not only reduces the number of animals sacrificed, but is also suitable for monitoring disease progression in live mice. Thus, our ultrasound imaging method may likely assist in the development of novel therapies that alleviate muscle injury induced by various respiratory diseases. Particularly, in clinical diagnoses of obstructive lung diseases, ultrasound imaging has the potential to be used in conjunction with other standard tests to detect the early onset of diaphragm muscle fatigue. In the current protocol, we describe how to accurately evaluate diaphragm contractility in a mouse model using a diagnostic ultrasound imaging technique.

Video Link

The video component of this article can be found at https://www.jove.com/video/51290/

Introduction

Recently, diagnostic ultrasound imaging techniques have been applied to mouse models of renovascular hypertension and pancreatic cancer[1,2]. However, these techniques have not been widely used in rodent respiratory muscle function assay. Therefore, we have developed a diagnostic ultrasound imaging method as a valuable tool for *in vivo* longitudinal assessments of diaphragm mobility in mice.

There are several advantages to diagnostic ultrasound imaging. For instance, it is noninvasive, safe, portable, and allows for real time measurements at a relatively low cost[3]. Particularly, certain low frequency ultrasound devices were able to detect air trapping, a clinical characteristic of chronic obstructive pulmonary disease (COPD) with mild to severe airflow limitation[4]. Thus, diagnostic ultrasound imaging may serve as an easily accessible and reproducible screening method for real-time monitoring of respiratory disorders.

Diagnostic ultrasound imaging techniques are frequently applied to larger animals or human subjects. However, there have been a limited number of ultrasound imaging studies on mouse models, which is likely due to the challenges of performing ultrasound on small-scale subjects. The current protocol outlines a novel procedure for measuring diaphragm function in the mouse. In addition, although there have been several rodent studies on diaphragm function, most of the results were generated by isolating muscle strips directly from the euthanized animal[5-7]. In contrast, using an *in vivo* diagnostic ultrasound imaging method for analyzing diaphragm activity would decrease the number of animals sacrificed for experimentation. Furthermore, long-term treatments focused on enhancing diaphragm contractility may be accurately assessed via ultrasound in rodent models without sacrificing animals.

In our lab, we have developed an effective method for visualizing as well as analyzing mouse diaphragm activity using an ultrasound machine, which helps the understanding of diaphragm function *in vivo*, avoids invasive methods to animals, and aids in the development of therapeutic treatments for respiratory dysfunction.

Protocol

All procedures involving animal subjects were approved and completed in accordance and compliance with The Ohio State University Institutional Animal Care and Use Committee (IACUC) regulations and guidelines.

1. Mouse Anesthesia

1. Set up a clean procedure table with a heated isothermal pad wrapped in a surgical towel. The heating pad should be maintained between 30 °C and 34 °C to stabilize the animal's core temperature while reducing potential stress to the animal.

2. Place the mouse in an anesthesia induction chamber with the following parameters: oxygen flow rate set to 1.5 L/min and isoflurane vaporizer set to 3.5%. Complete sedation should take place within 1-2 min. If an induction chamber is not available, a bell jar may be used with a wire mesh positioned at the bottom to avoid direct animal contact with the isoflurane.
3. Immediately remove the mouse from the induction chamber once it is completely anesthetized (achieved when the mouse loses voluntary motor function). Apply a nose-cone to the animal for maintenance of anesthesia. The oxygen flow rate should be reduced to approximately 0.5 L/min and the isoflurane vaporizer should be set within the range of 1.5 to 2.5%.
    1. Apply a small amount of ophthalmic ointment directly to the corneas to reduce eye dryness[8]. In addition, during anesthesia, the mouse should maintain an absence of the pedal withdrawal reflex, the mucous membranes should remain a pink color, and breathing should appear steady.

2. Preparing for Diagnostic Ultrasound Imaging Procedure

1. Restrain each leg of the mouse on the heated procedure table with a removable adhesive, such as surgical tape.
2. Using an electric razor, remove the hair on the ventral body surface between the abdomen and half way up the thoracic cavity. Apply hair removal cream to further remove the remaining hair that is not cut by the razor. Wipe off the cream with a damp gauze pad after 2-3 min.
3. Remove the excess hair using a water-moistened gauze pad and clean the shaved region with 70% alcohol or equivalent antiseptic. The ultrasound probe will be applied to this area to visualize diaphragm function. A topical analgesic may be provided to animals experiencing minor skin irritation due to hair removal.

3. Diagnostic Ultrasound Imaging Protocol

1. Turn on the ultrasound device and adjust the output power (if necessary) on the apparatus by percentage to obtain optimum resolution.
2. Set the ultrasound machine to either B (brightness)-mode, M (motion)-mode, or both before imaging, which allows for proper visualization of the mouse diaphragm contraction.
3. Apply a small amount of ultrasound gel on the mouse's upper abdomen and massage the gel toward the thoracic cavity.
4. Place the ultrasound transducer in this area and angle it upward towards the heart. Adjust the probe until an optimized resolution of the image is achieved. Note: for this protocol, a micro-convex array or linear phased array transducer is an ideal probe to use due to the small footprint and excellent axial resolution[9]; the frequency needs to be adjusted across the bandwidth and for these experiments a range of 6.5-12 MHz may be utilized.
5. Press the freeze button to temporarily save the diaphragm images and view the selected contractions.
6. Save the recording as a cine loop, which allows for later measurements of diaphragmatic excursion as well as respiration rate. Note: frames of images can be saved in the computer memory or on an external hard drive for future analysis[9].
    1. Precisely measure the depth of diaphragm movement from relaxation to contraction using the electronic calipers that are part of the ultrasound software.
    2. Convert the cine loop file into a MPEG file and determine the respiration rate by counting the number of diaphragmatic contractions during the recording period. Alternatively, the number of contractions per min (respiration rate) may be counted from the M-mode image.

4. Post Anesthesia Animal Recovery

1. The mouse should completely recover from anesthesia within 1 hour. Do not leave the animal unattended until it has regained sufficient consciousness to maintain sternal recumbency.

Representative Results

A typical ultrasound image of a mouse diaphragm is shown in **Figure 1A**. The mouse diaphragm maximal vertical displacement was recorded. This distance was calculated by precisely measuring the depth of diaphragm movement from relaxation to contraction using the electronic calipers that are part of the ultrasound software. **Table 1** displays these distance measurements of diaphragmatic contractions from three different mice. After converting the cine loop file into a MPEG file, the respiration rate was determined by counting the number of diaphragmatic contractions during a six second recording period. This analysis can be performed using B-mode. Alternatively, M-mode provides a visualized picture of diaphragm vertical motion as well as respiration rate as shown in **Figure 1B**. These results demonstrate that this method is effective in accurately observing mouse diaphragm contractions. Furthermore, by recording diaphragm function, this protocol also allows for assessing two important parameters including diaphragm excursion and respiration rate. This imaging method is useful for direct comparison between healthy and diseased diaphragm muscle. However, **Figure 2** demonstrates the potential imaging artifacts that may occur when performing diagnostic ultrasound imaging.
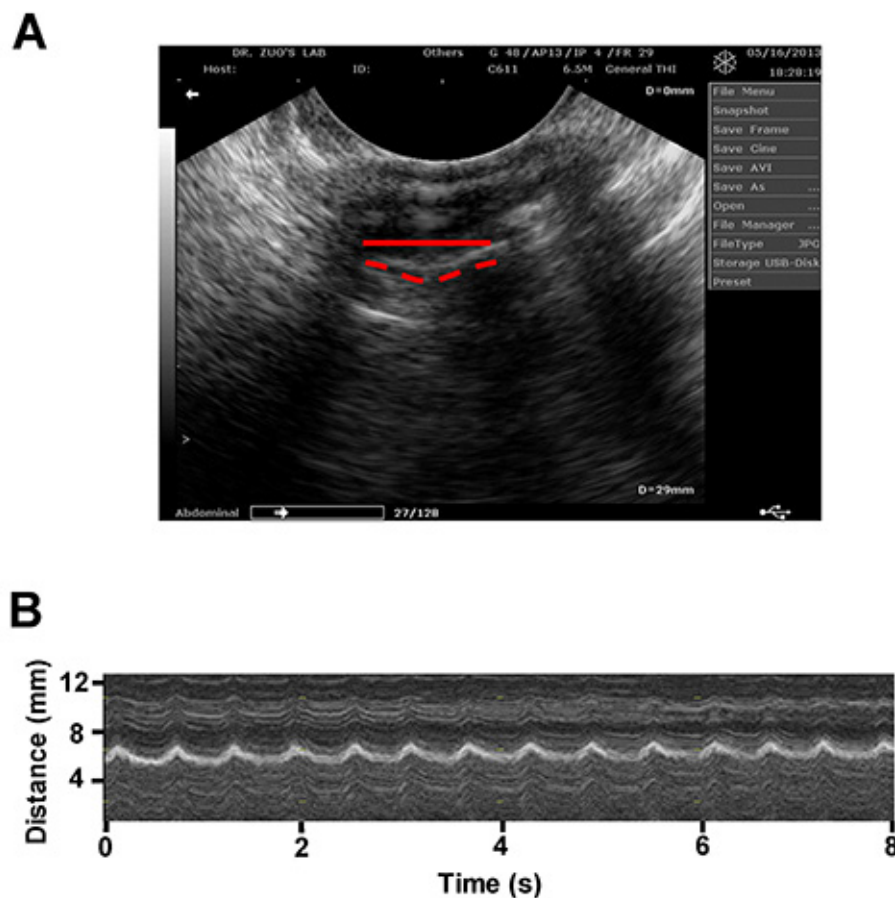
Figure 1. A. A representative ultrasound image of a mouse diaphragm muscle (B-mode). The solid and dashed lines depict the diaphragm during contracted and relaxed states, respectively. **B**. A representative ultrasound image of a contracting mouse diaphragm (M-mode). Please click here to view a larger version of this figure.
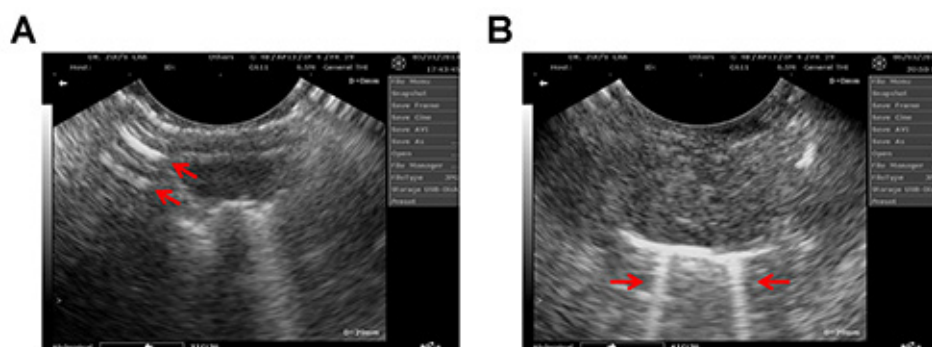

Figure 2. An ultrasound image of mouse diaphragm muscle with the presence of possible reverberation (**A**) and comet-tail (**B**) artifacts (indicated by the arrows). Please click here to view a larger version of this figure.

	1st measurement (mm)	2nd measurement (mm)	3rd measurement (mm)	Average (mm) ± SD
Mouse 1	0.96	0.92	1.06	0.980 ± 0.072
Mouse 2	0.93	0.99	1.01	0.977 ± 0.042
Mouse 3	0.91	0.93	0.89	0.910 ± 0.020

Table 1. Distance measurements of mouse diaphragm movement. Averages were calculated from three separate recorded values for each individual mouse. Standard deviation is defined as SD. Note, animal variance has no significant effect on the measurement of diaphragm contractions ($P = 0.1224$).

Discussion

The current experimental protocol develops diagnostic ultrasound imaging techniques specific to the diaphragm activity in a mouse model via a non-invasive, *in vivo* approach. The anesthesia apparatus settings are approximated values, which may be slightly adjusted for each animal since individual mice may respond differently to anesthesia. To prevent improper anesthesia administration, it is important to regularly monitor the mouse's vital signs including the heart rate, respiration rate, and body temperature. Furthermore, hair must be removed prior to ultrasound scanning because unshaved hair may blur the image and prevent accurate visualization of the diaphragm contractions.

We used B-mode ultrasound imaging to provide a two-dimensional (2D) cross sectional image of the mouse diaphragm and used M-mode to monitor diaphragm motion kinetics. It is important to use a micro-convex array transducer for 2D images because it provides improved axial resolution of superficially located anatomical structures compared to traditional linear array transducers[10]. It is also important to note that electronic focusing of the image degrades as the focal length is extended[9]. In addition, an adequate amount of ultrasound gel should be applied to the mouse's abdomen for acquiring distinct images. The gel limits the possibility of air pockets between the skin and the transducer to produce a high resolution image[11].

Although the application of diagnostic ultrasound imaging is promising, there are limitations to using this technique as a research tool. For instance, it is critical that the end user is well-trained in obtaining accurate and reproducible images and is able to interpret diaphragm activity consistently. Furthermore, mirror image artifacts occur when one anatomical structure, such as the diaphragm, is displayed twice on the monitor. This is considered a propagation artifact and results in the reflection being improperly located within the ultrasound operating system[12,13]. For example, ultrasound transducers can produce several off-axis beams which can reflect off an anatomical structure that is not in the pathway of the main beam[12,14]. Moreover, due to refraction, the beam may not always travel in a straight line from the reflector. Since the ultrasound can only process the signal that is returned to the transducer and cannot determine the timing of the refraction, the monitor may likely display the same anatomical structure twice at different distances and thus exhibit a mirror image artifact.

An additional propagation artifact that is encountered is reverberation. This artifact displays evenly spaced parallel lines that are generally positioned perpendicularly to the ultrasound beam (**Figure 2A**)[15]. This type of artifact may disrupt a true field of vision and mask specific anatomical structures of interest. Thus, caution should be taken when analyzing the data. A subset of reverberation artifact is the comet-tail or B-lines. These are a type of reverberation artifact that forms a vertical trajectory of dense echoes, extending from the diaphragm to the edge of the ultrasound screen[16] (as illustrated in **Figure 2B**). These artifacts are produced by multiple reflections that are occurring between or within a structure and the transducer[13], which can be minimized by angling the transducer to avoid a perpendicular contact with the specular objects[17]. Despite these limitations, diagnostic ultrasound imaging enables a safe, sensitive, and rapid analysis of diaphragm function in a mouse model, which can potentially evaluate rodent diaphragm dysfunction and help develop novel pre-clinical therapies for respiratory disorders.

Disclosures

The authors declare that they have no competing financial interests.

Acknowledgements

References

1. Snyder, C. S., *et al.* Complementarity of ultrasound and fluorescence imaging in an orthotopic mouse model of pancreatic cancer. *BMC Cancer*. **9**, 106, doi:10.1186/1471-2407-9-106 (2009).
2. Franchi, F., *et al.* Non-invasive assessment of cardiac function in a mouse model of renovascular hypertension. *Hypertension Research: Official Journal of the Japanese Society of Hypertension*, doi:10.1038/hr.2013.43 (2013).
3. Coatney, R. W. Ultrasound imaging: principles and applications in rodent research. *ILAR Journal / National Research Council, Institute of Laboratory Animal Resources*. **42**, 233-247 (2001).
4. Morenz, K., *et al.* Detection of air trapping in chronic obstructive pulmonary disease by low frequency ultrasound. *BMC Pulmonary Medicine*. **12**, 8, doi:10.1186/1471-2466-12-8 (2012).
5. Gilliam, L. A., Moylan, J. S., Ann Callahan, L., Sumandea, M. P., & Reid, M. B. Doxorubicin causes diaphragm weakness in murine models of cancer chemotherapy. *Muscle & Nerve*. **43**, 94-102, doi:10.1002/mus.21809 (2011).
6. Ferreira, L. F., Campbell, K. S., & Reid, M. B. Effectiveness of sulfur-containing antioxidants in delaying skeletal muscle fatigue. *Medicine and Science in Sports and Exercise*. **43**, 1025-1031, doi:10.1249/MSS.0b013e3182019a78 (2011).
7. Zuo, L., & Clanton, T. L. Reactive oxygen species formation in the transition to hypoxia in skeletal muscle. *American Journal of Physiology. Cell Physiology*. **289**, C207-216, doi:10.1152/ajpcell.00449.2004 (2005).
8. Helms, M. N., Torres-Gonzalez, E., Goodson, P., & Rojas, M. Direct tracheal instillation of solutes into mouse lung. *J. Vis. Exp.* e1941 (2010).
9. Hedrick, W. R., Hykes, D. L., & Starchman, D. E. *Ultrasound Physics and Instrumentation*. 4th edn, 445 Elsevier Mosby (2005).
10. von Sarnowski, B., Khaw, A. V., Kessler, C., & Schminke, U. Evaluation of a microconvex array transducer for the ultrasonographic examination of the intrathoracic segments of the supraaortic arteries. *Journal of Neuroimaging: Official Journal of the American Society of Neuroimaging*. **20**, 246-250, doi:10.1111/j.1552-6569.2009.00360.x (2010).
11. Stocksley, M. *Abdominal Ultrasound*. 7-8 Cambridge University Press (2001).
12. Kremkau, F. W., & Taylor, K. J. Artifacts in ultrasound imaging. *Journal of Ultrasound in Medicine: Official Journal of the American Institute of Ultrasound in Medicine*. **5**, 227-237 (1986).

13. Kremkau, F. W. *Diagnostic Ultrasound: Principles and Instruments*. 7th edn, 521 Saunders Elsevier (2006).
14. Laing, F. C., & Kurtz, A. B. The importance of ultrasonic side-lobe artifacts. *Radiology*. **145**, 763-768 (1982).
15. Abu-Zidan, F. M., Hefny, A. F., & Corr, P. Clinical ultrasound physics. *Journal of Emergencies, Trauma, and Shock*. **4**, 501-503, doi:10.4103/0974-2700.86646 (2011).
16. Gargani, L. Lung ultrasound: a new tool for the cardiologist. *Cardiovascular Ultrasound*. **9**, 6, doi:10.1186/1476-7120-9-6 (2011).
17. Sanders, R. C., & Winter, T. *Clinical Sonography A Practical Guide*. 4th edn, 632 Lippincott Williams & Wilkins (2007).